The XMM-LSS Survey: SEDs of the hard AGN population

L.Maraschi (INAF/Brera), M. Polletta (IAP), G. Trinchieri, M. Giorgetti, M. Tajer (INAF/Brera), L. Chiappetti (INAF/IASF-MI) and the XMM-LSS collaboration

We present an XMM/CFHTLS/SPITZER study of the AGN detected in the 2-10keV band in the central part of the XMM-LSS survey (XMDS). The multi-frequency coverage enables a very high identifcation rate (>90%, 100% in the area covered by SWIRE) and yields well sampled spectral energy distributions. We have developed an efficient SED fitting procedure, which allows a reliable classification and photometric redshiftsto be determined with unprecedented accuracy for AGN. The IR-to-X-ray SED properties of the different classes appear to change continuously from AGN1 to SEY1.8 to AGN 2 to StarForming objects. We find a large population of optically obscured AGN (i.e. objects with SEDs fitted by AGN 2 or star forming galaxy templates). The stacked X-ray spectra of AGN type 2 and SF SEDs are harder than those of AGN type1/Sey1.8, and close to that of the XRB. The fraction of optically obscured AGN decreases with increasing luminosity/redshift while the fraction of X-ray absorbed AGN does not change significantly, suggesting a decoupling of gas and dust in the close environment of AGN at high luminosities.

The XMM-Newton Medium Deep Survey (2^h 26^m, -4° 30′) (XMDS; Chiappetti et al. 2005)

DATA SETS

XMM-Newton:
18 x 20 ks (2.6 deg² at F(2-10 keV) ≥10^{-14} cgs)
Spitzer (SWIRE: Lonsdale et al. 2003):
IRAC (3.6, 4.5, 5.8, 8.0 μm)
5σ-limit: 4.3, 8.3, 58.5, 65.7 μJy
MIPS (24, 70, 160 μm)
5σ-limit: 0.24, 17, 105 mJy
Optical & near-IR (VVDS: PI: O. Le Fevre)
U (25.4), B (26.5), R(26.2), I(25.0) [AB]
J (24.2); K (23.9) [AB]
Optical (CFHTLS d1+w1):
U (25.5), g′ (25.6), r′ (25.7), i′ (25.5), z (24.0) [AB]
UKIDSS near-IR
J (24.8), K (25.9) [AB] (0.6 deg²)
VLA (20 cm) (Bondi et al. 2003; Ciliegi et al. 2005):
20cm (80 μJy 5 sigma)
Spectroscopy (LeFevre et al. 2005; Gavignaud et al. 2006 Lacy et al. 2006; Garcet et al. 2007)

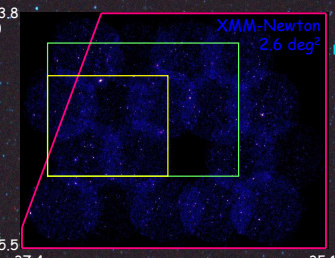

SAMPLE
136 X-ray sources (2 clusters)
Field: 1 deg2 (green area in Fig. 1)
122 w/ unique opt. counterpart
9 w/ dubious optical counterpart
3 opt. blank
121 w/ SWIRE coverage
121 detected at 3.6 and 4.5μm, 87 at 24μm)
66 w/ UKIDSS JK
32 w/ radio counterpart
11 spectroscopic redshifts

Fig. 1: Layout of the XMDS survey. Background image: 18 XMM-Newton pointings. Green rectangle: VVDS survey (1 deg²) Magenta area: SWIRE Yellow rectangle:UKIDSS (0.6 deg2) .

Photometric redshifts and classification

Our fitting procedure yields AGN redshifts with unprecedented accuracy (15% outliers) (Polletta et al., 2007- Bolzonella et al. 2000)

➪ SED classification results: 40% of AGN1, 40% of AGN2, 19% of SF.

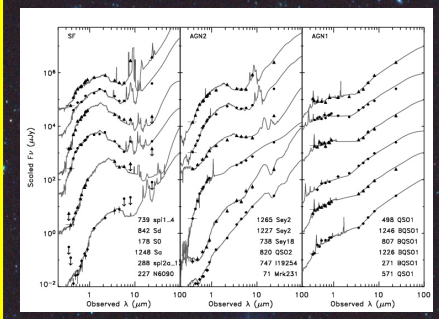

Fig. 2: Examples of different types of SEDs: 6 SF (left panel), 6 AGN2 (middle panel), and 6 AGN1 (right panel).

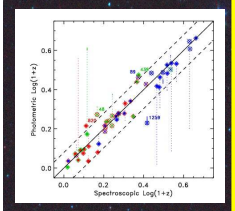

Fig. 3: spectroscopic versus photometric redshifts

Multi-wavelength average properties of the AGN classes

The SED properties of the different classes appear to change continuously from AGN1 to SEY1.8 to AGN 2 to SF:
Ł the optical-UV continua become increasingly red and the X-ray spectra increasingly hard along the classification sequence based on the optical -IR photometry

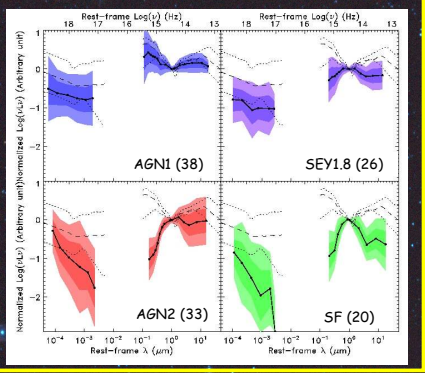

Fig. 4: Median rest-frame SEDs (points connected by solid lines) normalized at 1μm with 1 and 2 sigma dispersion (colored regions) Dashed and dotted curves represent the median and ±90% dispersion respectively of the QSO templates (Elvis et al. 1994).

Spectral slopes of stacked data for different AGN classes

The slopes of the type 2 and SF AGN classes are significantly flatter than those of AGN 1 + Sey 1,8 and close to the XRB spectrum

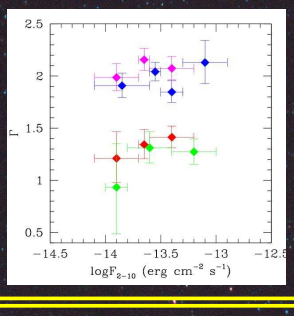

Fig. 5: Photon indexes for
BLUE: AGN1
PURPLE: Sey 1.8
RED:AGN2
GREEN:SF

X-ray Absorption

It appears that high values of N_h appear for AGN 1 as well as for AGN2 and SF

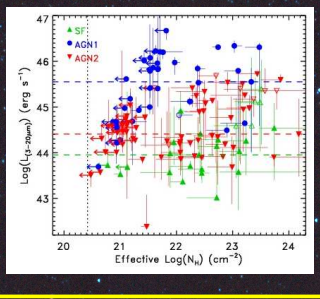

Fig. 6 Broad band infrared luminosity versus N_h estimated from X-ray data

The X-ray absorbed fraction appears to increase with decreasing flux but not to depend on luminosity (or redshift, not shown)
Optical obscuration instead is more frequent in low luminosity sources (not shown)

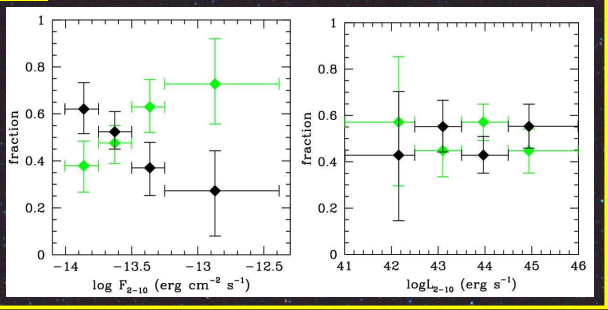

Fig. 7 Fraction of X-ray absorbed (black) and unabsorbed (green) AGNs versus X-ray flux and luminosity

Summary & Conclusions

1. The XMDS hard X-ray selected AGN sample is divided in three groups based on their optical-IR SED: 40^{+3}_{-6}% AGN1, 40^{+10}_{-7}% AGN2, 19^{+8}_{-6}% SF (Sey 1.8 are included in type2 AGN):. A comparison with similar samples from the literature indicates a decreasing fraction of AGN1s at fainter flux limits (Franceschini et al. 2005). The AGN1 fraction is lower and the AGN2 fraction is higher than in similarly selected spectroscopically classified samples (Eckart et al. 2006; Perola et al. 2004). Note however that the limit between type 1 and type 2 objects is blurred by the "Sey 1.8"class.

2. Average SED properties: The SED properties are remarkably continuous along the classification sequence. The average SED of AGN1 is dominated by the AGN emission from optical to IR, with a small fraction of X-ray absorbed spectra. AGN1 with the bluest optical spectra are also the reddest in the mid-IR, suggesting a decreasing contribution of the host galaxy. In AGN2, dust emission associated with the AGN is detected in the mid-infrared, and emission from the host galaxy becomes increasingly important in the optical. The AGN2 class shows a broad range of X-ray properties, with the majority being absorbed in the X rays. Sources classified as SF do not show any AGN signature at optical or IR wavelengths, are absorbed in the X rays and have a stacked X-ray spectrum close to that of the background.

3. Dust properties vs X-ray luminosity and AGN classification: The mid-IR/X-ray luminosity ratio is characterized by a broad dispersion, but it is on average constant for AGN1 and AGN2 and independent of the X-ray luminosity, while some SF show extremely low values.

4. The nature of elusive AGN: AGN in the SF class are elusive AGNs at optical and IR wavelengths, similarly to XBONGs (Comastri et al. 2002), and IR-selected AGNs with blank optical spectra (Martinez-Sansigre et al. 2006; Lacy et al. 2006). The properties of these sources are explained by large obscuration in the mid-IR, however it is not clear whether the large obscuration is an effect of orientation or whether it implies a dust distribution either more extended or with a larger inner radius (see e.g. Ballantyne et al. 2006).

References

Ballantyne, D.R. et al. 2006, ApJ, 639, 740
Bolzonella, M. et al. 2000, A&A, 363, 476
Bondi, M. et al. 2003, A&A, 403, 857
Chiappetti, L. et al. 2005, A&A, 439, 413
Ciliegi, P. et al. 2005, A&A, 441, 879
Comastri, A. et al. 2002 [astro-ph/0203019]
Eckart, M. et al. 2006, ApJS, 165, 19
Elvis, M. et al. 1994, ApJS, 95, 1
Franceschini, A. et al. 2005, 2005, AJ, 129, 2074
Garcet, O. et al. 2007, A&A submitted
Gavignaud, L. et al. 2006, A&A, 457, 79
Lacy, M. et al.z2006, AJ accepted [astro-ph/0609594]
Le Fevre, O. et al. 2005, A&A, 439, 845
Lonsdale, C. J. et al. 2003, PASP, 115, 897
Martinez-Sansigre, A. et al. 2006, MNRAS, 370, 1479
Perola, G.C. et al. 2004, A&A, 421, 491
Polletta, M., Tajer, M., Maraschi, L. et al. 2007, ApJ, 663
Tajer, M., Polletta, M., Maraschi, L. et al. 2007, A&A, in press

Acknowledgments This work is based on observations made with the Spitzer Space Telescope, which is operated by the Jet Propulsion Laboratory, California Institute of Technology under NASA contract 1407. Support for this work, part of the Spitzer Space Telescope Legacy Science Program, was provided by NASA through an award issued by the Jet Propulsion Laboratory, California Institute of Technology under NASA contract 1407. The INAF members of the team acknowledge financial contribution from contract ASI-INAF I/023/05/0. Center). Based on observations obtained with MegaPrime/MegaCam, a joint project of CFHT and CEA/DAPNIA, at the Canada-France-Hawaii Telescope (CFHT) which is operated by the National Research Council (NRC) of Canada, the Institut National des Science de l'Univers of the Centre National de la Recherche Scientifique (CNRS) of France, and the University of Hawaii. This work is based in part on data products produced at TERAPIX and the Canadian Astronomy Data Centre as part of the Canada-France-Hawaii Telescope Legacy Survey, a collaborative project of NRC and CNRS. Backgroung image: 3-color image of 1 deg2 area of the XMDS (blue: 3.6μm, green: 4.5μm; red: 8μm)